Korean J. Chem. Eng., 33(9), 2711-2715 (2016)
DOI: 10.1007/s11814-016-0151-1

pISSN: 0256-1115
eISSN: 1975-7220

Effect of oxygen flow rate on the electrical and optical characteristics of dopantless tin oxide films fabricated by low pressure chemical vapor deposition

Jun-Hyun Kim*, Hae-Min Lee, Doo Won Kang***, Kyung Mi Lee***, and Chang-Koo Kim*,†**

*Department of Chemical Engineering and Department of Energy Systems Research, Ajou University, 206 Worldcup-ro, Yeongtong-gu, Suwon 16499, Korea
**Institute of NT-IT Fusion Technology, Ajou University, 206 Worldcup-ro, Yeongtong-gu, Suwon 16499, Korea
***Smart Electronics, 87 Samdong-ro, Samdong-myeon, Ulju-goon, Ulsan 44956, Korea
(*Received 25 April 2016 • accepted 6 June 2016*)

Abstract−The effect of oxygen flow rate on the electrical and optical characteristics of dopantless tin oxide films prepared by low pressure chemical vapor deposition (LPCVD) was investigated. A decrease in the sheet resistance of the film with increasing oxygen flow rate in the range of 200-300 sccm was attributed to an increase in the film thickness (and correspondingly, in the grain size); while at oxygen flow rates higher than 300 sccm, the increase in the sheet resistance of the film resulted from an increase in the X-ray diffraction peak intensities of the (110), (101), and (201) planes. The optical bandgap of the film decreased when the oxygen flow rate was increased from 200 to 300 sccm, but it remained nearly constant for oxygen flow rates higher than 300 sccm. A maximum figure-of-merit was achieved for films prepared with an oxygen flow rate of 300 sccm.

Keywords: LPCVD, Dopantless, Tin Oxide, Sheet Resistance, Optical Bandgap, Figure of Merit

INTRODUCTION

Tin oxide (SnO_2) has drawn much attention for its high electrical conductivity, high optical transparency in the visible wavelength region, high reflectivity in the infrared wavelength region and good mechanical and chemical stability [1-5]. Tin oxide is an n-type semiconductor with tetragonal rutile structure, where oxygen vacancies give rise to charge carriers. Thus, tin oxide films have potential applications in transparent conducting electrodes, solar cells, gas sensors, flat panel displays and heat reflection coatings [6-13]. These applications require a precise control of the electrical and optical properties of tin oxide films tailored for the specific application.

Different deposition methods, such as sputtering, evaporation, spray pyrolysis, and chemical vapor deposition (CVD), have been used to prepare tin oxide films [1-4,14-18]. Among these methods, the CVD process is relatively simple, inexpensive, and affords a good control over the film properties. Particularly, low pressure chemical vapor deposition (LPCVD) has the advantage of producing films of uniform thickness with low impurity concentrations.

Electrical properties (e.g., sheet resistance) of tin oxide films are usually varied by introducing dopants such as fluorine and antimony into the film. However, these dopants are detrimental to the environment. Recently, we reported the preparation of dopantless tin oxide films grown by LPCVD, where we investigated the effects of the deposition temperature on the film properties [19].

As an extension of our previous work, this study reports on the electrical and optical characteristics of dopantless tin oxide films deposited by LPCVD with different flow rates of oxygen. The oxygen flow rates ranged from 200 to 500 sccm. The changes in the sheet resistance and the optical bandgap of the films were analyzed by the modification of crystallography and surface morphology of the films.

EXPERIMENTAL

LPCVD of tin oxide films was performed in a horizontal hot-wall reactor system, which was described in detail in a previous report [19]. Tin oxide films were deposited on Si substrates. The substrate was a p-type Si (100) wafer that was cut into a 10×10 mm^2 square.

Dibutyl tin diacetate (DBTDA, $C_{12}H_{24}O_4Sn$) and oxygen were used as tin source and oxidant, respectively. Tin oxide films were formed by the following reaction:

$$C_{12}H_{24}O_4Sn+17O_2 \rightarrow SnO_2+12CO_2+12H_2O \quad (1)$$

DBTDA is a liquid at ambient conditions and therefore argon was used as a carrier gas to transport the vaporized DBTDA to the reaction chamber. The flow rate of argon was 50 sccm. The chamber pressure and the deposition temperature were fixed at 4 Torr and 450 °C, respectively. The oxygen flow rate was varied from 200 to 500 sccm to investigate its effect on the electrical and optical characteristics of the tin oxide films.

The thickness of the tin oxide film was measured with a thickness meter (K-Mac, Spectra Thick 2000). The sheet resistance was measured by using a four-point probe (Advanced Instrument Technology, CMT-SR1000N). Optical absorption of the film was measured by using a UV-VIS spectrometer (Jasco, V-650). Surface

†To whom correspondence should be addressed.
E-mail: changkoo@ajou.ac.kr

morphology of the tin oxide films was examined by field emission scanning electron microscopy (FE-SEM, JEOL, S-4800). Microstructural analysis of the film involved using a high power X-ray diffractometer (XRD, Rigaku, Ultima III), which used a CuKα radiation (wavelength=0.154 nm) as an incident beam.

RESULTS AND DISCUSSION

Fig. 1 shows the deposition rates of the tin oxide films deposited at various flow rates of oxygen. The deposition time was 1 h in all cases. The deposition rate monotonically increases from 326 to 554 nm/h as the oxygen flow rate increases from 200 to 300 sccm before reaching a plateau for flow rates higher than 300 sccm. This behavior of the deposition rate with respect to the oxygen flow rate is similar to results from other studies on the LPCVD of tin oxide films using other precursors such as tetramethyl tin (TMT) and tin tetrachloride ($SnCl_4$) [20].

The CVD of tin oxide films is a heterogeneous reaction during which gaseous reactants react with a solid substrate. A heterogeneous reaction is generally controlled by either the mass transfer of reactants to the substrate surface or by a surface reaction, depending on the process conditions. In the present study, an increase in the deposition rate of the tin oxide films with oxygen flow rate up to 300 sccm implies that the deposition is limited by mass transfer in this regime. With increasing flow rates of oxygen, the mass transfer coefficient increases. At oxygen flow rates higher than 300 sccm, mass transfer is sufficiently faster than the surface reaction, resulting in a nearly constant deposition rate with oxygen flow rate. Therefore, the deposition is limited by surface reaction in this regime.

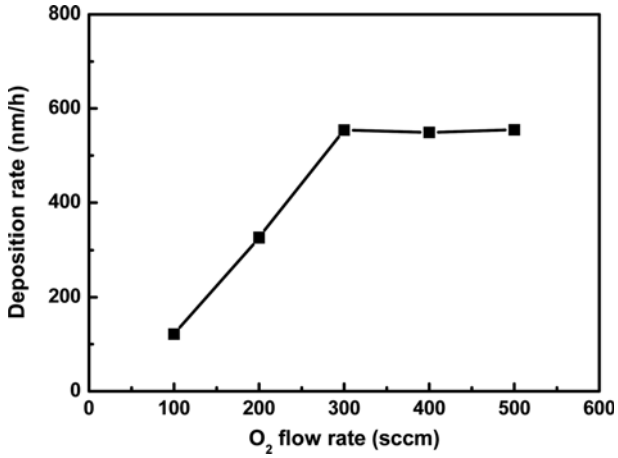

Fig. 1. Deposition rate of tin oxide films at different flow rates of oxygen.

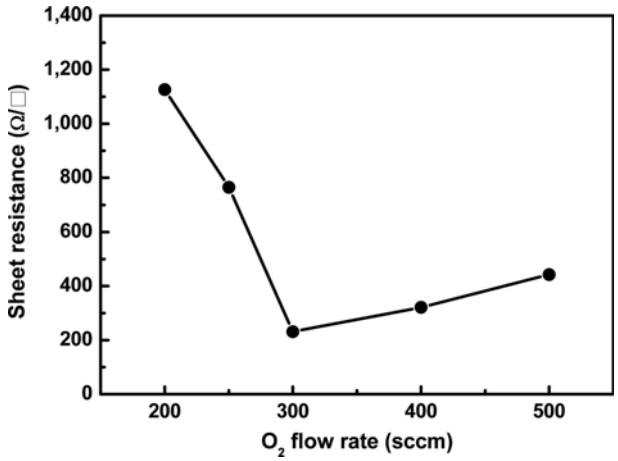

Fig. 2. Sheet resistance of tin oxide films as a function of oxygen flow rate.

Fig. 2 shows the sheet resistance of the tin oxide films as a function of oxygen flow rate. The sheet resistance of the film drastically decreases from 1,126 to 272 Ω/□ as the oxygen flow rate increases from 200 to 300 sccm. For oxygen flow rates higher than 300 sccm, the sheet resistance is increased to 442 Ω/□. It is known that the electrical conductivity of tin oxide films increases with film thickness because of an increase in grain sizes and a corresponding decrease in the number of grain boundaries [1]. Therefore, a decrease in sheet resistance of the tin oxide films with increasing oxygen flow rate up to 300 sccm results from an increase in the film thickness. However, the sheet resistance of the film increased for oxygen flow rates higher than 300 sccm even though the film thickness was nearly constant with oxygen flow rate in this range (see Fig. 1). This implies that factors other than film thickness affect the sheet resistance of tin oxide films at high oxygen flow rates (higher than 300 sccm).

The dependence of grain size on the film thickness can also be determined from SEM images. Fig. 3 shows SEM images of the tin oxide films deposited at various flow rates of oxygen. The average grain size increases from 50 to 100 nm with oxygen flow rates of 200-300 sccm, and the films deposited at oxygen flow rates of 300-500 sccm show no discernible change in grain size. This result is in accordance with the change in the film thickness with oxygen flow rate.

To explain the reason why the dependence of sheet resistance of the tin oxide film on the oxygen flow rates higher than 300 sccm did not follow that of the grain size, microstructural analysis was undertaken. Fig. 4 shows the X-ray diffraction (XRD) patterns of the tin oxide films prepared by LPCVD at various flow rates of oxygen. For all the different oxygen flow rates, the diffraction patterns of the tin oxide films show only SnO_2 peaks corresponding to the (110), (101), (200), (211), and (220) planes. At all flow rates of oxygen, the tin oxide films show the (200) plane as the preferred orientation. This agrees with other studies on CVD of the tin oxide films using DBTDA as a tin source [21]. The intensity of the (200) peak increases slightly with oxygen flow rate. In contrast, the intensities of the peaks other than the (200) plane show no discernible changes with oxygen flow rate in the 200-300 sccm range. The intensity of the (110) peak starts to increase with oxygen flow rate higher than 300 sccm and the intensities of the (101) and (211) peaks also increase with oxygen flow rate higher than 400 sccm. This structural variation of the film can explain why the sheet resistance of the tin oxide films increases with oxygen flow rate in the 300-500 sccm range. It has been found that films grown along planes other than the (200) plane produce deep-lying trapping centers, which decreases the concentration of charge carriers, leading to a corresponding reduction in the conductivity of the film [21]. There-

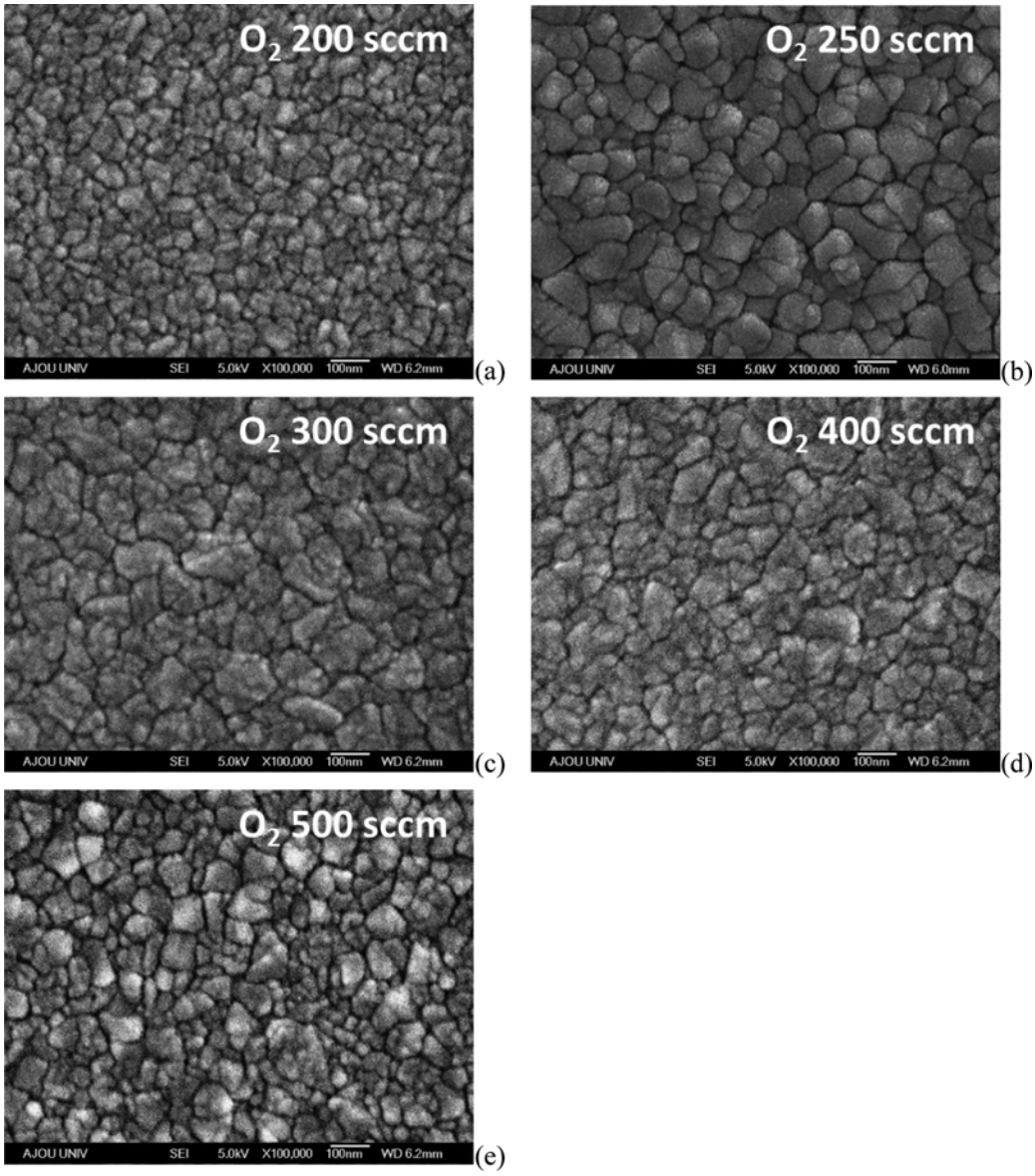

Fig. 3. SEM images of tin oxide films deposited at oxygen flow rates of (a) 200, (b) 250, (c) 300, (d) 400, and (e) 500 sccm.

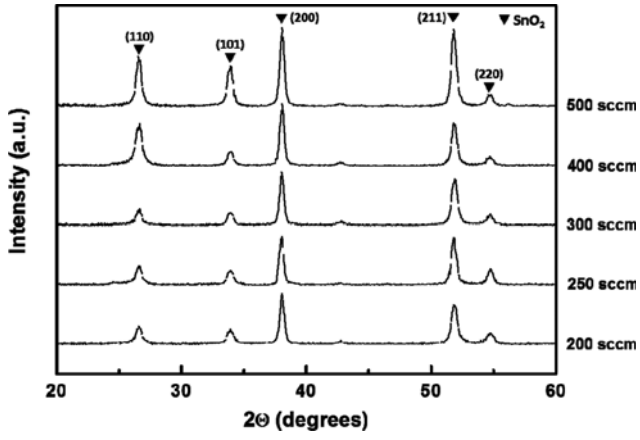

Fig. 4. XRD patterns of tin oxide films prepared with different flow rates of oxygen.

fore, the sheet resistance of the tin oxide films increases with oxygen flow rate in the 300-500 sccm range due to increased crystal growth for the (110), (101), and (211) planes as shown by the XRD results.

Optical absorption measurements were conducted to investigate the dependence of the optical bandgap of the tin oxide films on the oxygen flow rate. The optical bandgap of the film was obtained using the relationship between the absorption coefficient and the photon energy. It is known from previous work that tin oxide with the rutile structure has a direct bandgap [22]. For a film with a direct bandgap, the absorption coefficient is given by the following equation:

$$(\alpha h\nu)^2 = B(h\nu - E_g) \quad (2)$$

In Eq. (2), a is the absorption coefficient, E_g is the optical bandgap, B is a constant, and $h\nu$ is the photon energy where h is the Planck's constant and ν is the frequency. Since $(\alpha h\nu)^2$ has a linear

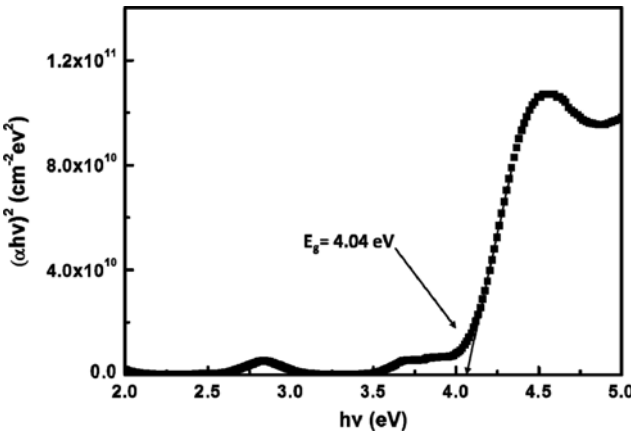

Fig. 5. Plot of $(\alpha h\nu)^2$ vs. $h\nu$ to estimate the optical bandgap by extrapolating the linear part of the curve. The flow rate of oxygen is 200 sccm.

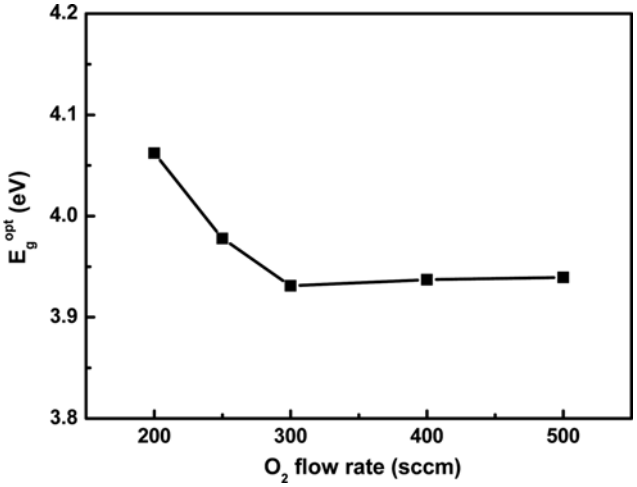

Fig. 6. Optical bandgap of tin oxide films as a function of oxygen flow rate.

relation with $h\nu$, the optical bandgap can be estimated by extrapolating the linear portion of the graph of $(\alpha h\nu)^2$ vs. $h\nu$ to $(\alpha h\nu)^2=0$. Fig. 5 shows a representative curve of $(\alpha h\nu)^2$ vs. $h\nu$ to calculate the optical bandgap of tin oxide film. In this figure, the flow rate of oxygen is 200 sccm. A linear fit of the curve in the photon energy range of 4.0-4.5 eV is used to estimate the optical bandgap from the intercept of the straight line on the x-axis (Fig. 5).

The optical bandgaps of the tin oxide films deposited with different flow rates of oxygen are calculated using the above-mentioned procedure and are shown in Fig. 6. As can be seen, the optical bandgap decreases as the oxygen flow rate increases from 200 to 300 sccm. For oxygen flow rates higher than 300 sccm, the bandgap remained almost unchanged. It has been reported that the optical bandgap of tin oxide films decreases with increasing film thickness [17]. Therefore, it can be concluded that a decrease in the optical bandgap with increasing oxygen flow rates of 200-300 sccm results from an increase in the thickness of the film, while a constant optical bandgap with oxygen flow rates higher than 300 sccm results from a constant film thickness.

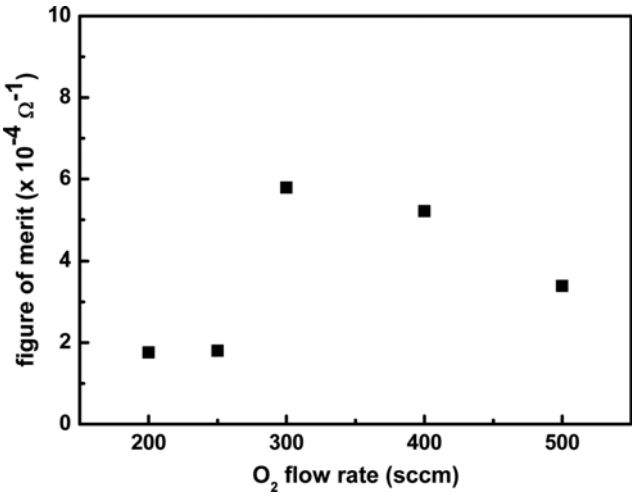

Fig. 7. Figure-of-merit for tin oxide films as a function of oxygen flow rate.

One of the most interesting applications of tin oxide is in transparent conducting electrodes. For the practical use of tin oxide films as a transparent conducting electrode, both the conductivity and transmittance of the films need to be as high as possible. In general, these are inversely related to each other [1]. The optimum values of these two parameters (conductivity and transmittance) can be considered together by introducing a parameter of a 'figure of merit'. For transparent conducing films, the figure of merit is defined as [23]

$$\Phi_{TC}=Tr^{10}/R_{sh} \quad (3)$$

where Tr is the transmittance at a particular wavelength and R_{sh} is the sheet resistance of the film. Fig. 7 shows the figure of merit of the tin oxide films deposited at various flow rates of oxygen. In this figure, the transmittance of the film was measured at the wavelength of 600 nm. The figure of merit has maximum value of 6×10^{-4} □/Ω when the oxygen flow rate is 300 sccm. This implies that under the process conditions used in this work, the tin oxide film deposited with an oxygen flow rate of 300 sccm has the best performance as a transparent conducting electrode.

CONCLUSIONS

Dopantless tin oxide films were prepared at different flow rates of oxygen by LPCVD, and the electrical and optical characteristics of the films were investigated. Changes in the deposition rate of the tin oxide films with oxygen flow rates revealed that the film deposition was limited by mass transfer for oxygen flow rates from 200 to 300 sccm and by surface reaction for higher flow rates (300 to 500 sccm).

Sheet resistance of the tin oxide films decreased as the oxygen flow rate increased from 200 to 300 sccm due to an increase in the film thickness and a corresponding increase in the grain size as verified by SEM measurements. Although the film thickness was nearly constant for oxygen flow rates higher than 300 sccm, the sheet resistance of the film increased with oxygen flow rate in this range. This was because of higher grain sizes as demonstrated by

the increase in the peak intensities of the (110), (101), and (201) planes in the XRD for oxygen flow rates in the 300-500 sccm range.

The optical bandgap of the tin oxide films decreased when the oxygen flow rate was increased from 200 to 300 sccm, and was nearly constant for higher oxygen flow rates, which is due to the dependence of the film thickness on the oxygen flow rate. The figure-of-merit of the tin oxide film, which is a measure of the superior performance of a transparent conducting electrode, had a maximum value when the oxygen flow rate was 300 sccm.

This work demonstrates that LPCVD is well adapted to the fabrication of dopantless tin oxide films and enables the optimization of the electrical and optical properties by controlling process parameters such as oxygen flow rate.

ACKNOWLEDGEMENT

This work was supported by the National Research Foundation of Korea (NRF) grant funded by the Korea government (MEST) (Grant Nos. 2015R1A2A2A01002305 and NRF-2009-0094046), and by the Advanced Manufacturing Technology Center (ATC) (Grant No. 10039034).

REFERENCES

1. F. J. Yusta, M. L. Hitchman and S. H. Shamlian, *J. Mater. Chem.*, **7**, 1421 (1997).
2. R. Y. Korotkov, P. Ricou and A. J. E. Farran, *Thin Solid Films*, **502**, 79 (2006).
3. M. Maleki and S. M. Rozati, *Phys. Scr.*, **86**, 015801 (2012).
4. S. Bansal, D. K. Pandya, S. C. Kashyap and D. Haranath, *J. Alloy. Compd.*, **583**, 186 (2014).
5. Y. Wang, I. Ramos and J. J. Santiago-Avilés, *J. Appl. Phys.*, **102**, 093517 (2007).
6. J.-Y. Kim, E.-R. Kim, Y.-K. Han, K.-H. Nam and D.-W. Ihm, *Jpn. J. Appl. Phys.*, **41**, 237 (2001).
7. D. W. Sheel, H. M. Yates, P. Evans, U. Dagkaldiran, A. Gordijn, F. Finger, Z. Remes and M. Vanecek, *Thin Solid Films*, **517**, 3061 (2009).
8. A. Klein, C. Korber, A. Wachau, F. Sauberlich, Y. Gassenbauer, S. P. Harvey, D. E. Proffit and T. O. Mason, *Materials*, **3**, 4892 (2010).
9. Y.-G. Kang, H.-J. Kim, H.-G. Park, B.-Y. Kim and D.-S. Seo, *J. Mater. Chem.*, **22**, 15969 (2012).
10. G. F. Fine, L. M. Cavanagh, A. Afonja and R. Binions, *Sensors*, **10**, 5469 (2010).
11. G. Korotcenkov, V. Brinzari, J. Schwank, M. DiBattista and A. Vasiliev, *Sens. Actuators B*, **77**, 244 (2001).
12. A. A. Yadav, E. U. Masumdar, A. V. Moholkar, M. Neumann-Spallart, K. Y. Rajpure and C. H. Bhosale, *J. Alloy. Compd.*, **488**, 350 (2009).
13. Y.-S. Cho, J. W. Moon, D. C. Lim and Y. D. Kim, *Korean J. Chem. Eng.*, **30**, 1142 (2013).
14. I. H. Kim, J. H. Ko, D. Kim, K. S. Lee, T. S. Lee, J.-H. Jeong, B. Cheong, Y.-J. Baik and W. M. Kim, *Thin Solid Films*, **515**, 2475 (2006).
15. V. Senthilkumar and P. Vickraman, *P. J. Mater. Sci.: Mater. Electron*, **21**, 578 (2010).
16. X. Q. Pan, L. Fu and J. E. Dominguez, *J. Appl. Phys.*, **89**, 6056 (2001).
17. R. K. Nath and S. S. Nath, *Sensor Mater.*, **21**, 95 (2009).
18. M.-M. Bagheri-Mohagheghi and M. Shokooh-Saremi, *Semicond. Sci. Technol.*, **19**, 764 (2004).
19. J.-H. Kim, S.-W. Cho, D. K. Kang, K. M. Lee, C. Y. Baek, H.-M. Lee and C.-K. Kim, *Sci. Adv. Mater.*, **8**, 117 (2016).
20. C. F. Wan, R. D. McGrath, W. F. Keenan and S. N. Frank, *J. Electrochem. Soc.*, **136**, 1459 (1989).
21. D. Belanger, J. P. Dodelet, B. A. Lombos and J. I. Dickson, *J. Electrochem. Soc.*, **132**, 1398 (1985).
22. K. L. Chopra, S. Major and D. K. Pandya, *Thin Solid Films*, **102**, 1 (1985).
23. G. Haacke, *J. Appl. Phys.*, **47**, 4086 (1976).